Phase-dependent light propagation in atomic vapors

Sarah Kajari-Schröder,[1] Giovanna Morigi,[2] Sonja Franke-Arnold,[3,4] and Gian-Luca Oppo[4]
[1] *Abteilung Quantenphysik, University of Ulm, D-89069 Ulm, Germany*
[2] *Grup d'Optica, Departament de Fisica, Universitat Autonoma de Barcelona, 08193 Bellaterra, Spain*
[3] *Department of Physics, University of Glasgow, Glasgow, Scotland, U.K.*
[4] *Department of Physics, University of Strathclyde, G14 0NG Glasgow, Scotland, U.K.*
(Dated: May 24, 2006)

Light propagation in an atomic medium whose coupled electronic levels form a ♢-configuration exhibits a critical dependence on the input conditions. In particular, the relative phase of the input fields gives rise to interference phenomena in the electronic excitation whose interplay with relaxation processes determines the stationary state. We integrate numerically the Maxwell-Bloch equations and observe two metastable behaviors for the relative phase of the propagating fields corresponding to two possible interference phenomena. These phenomena are associated to separate types of response along propagation, minimize dissipation, and are due to atomic coherence. These behaviors could be studied in gases of isotopes of alkali-earth atoms with zero nuclear spin, and offer new perspectives in control techniques in quantum electronics.

I. INTRODUCTION

Recent experimental progress demonstrates that the nonlinear optical properties of laser-driven atomic gases exhibit counter-intuitive features with promising applications. A peculiarity of these media, in fact, is the possibility to manipulate their internal and external degrees of freedom with high degree of control. Few recent and significative examples include the control of the internal dynamics by means of electromagnetically induced transparency (EIT) in an atomic vapor [1] (used for the generation of four-wave mixing dynamics [2]) and of controlled quantum pulses of light [3, 4]. In another experiment, the interplay of internal and external degrees of freedom in an ultracold atomic gas by means of recoil-induced resonances [5] was used to achieve waveguiding of light [6]. In this perspective, it is important to identify further possible control parameters on the atomic dynamics for the manipulation of the non-linear optical response of the medium.

Recent studies have been focusing onto the dynamics of light interacting with atoms with coupled electronic levels in a so-called 'closed-loop' configuration [7, 8]. In this configuration a set of atomic states is (quasi-) resonantly coupled by laser fields so that each state is connected to any other via two different paths of coherent photon-scattering. In these systems, the relative phase between the transitions critically influences dynamics [7] and steady states [8, 9, 10]. Applications of closed-loop configurations to nonlinear optics have featured double-Λ systems where two stable or metastable states are -each- coupled to two common excited states. A rich variety of nonlinear optical phenomena has been predicted [9, 11, 12] and experimentally observed [2, 13, 14, 15, 16, 17]. In [17], in particular, it has been shown experimentally that the properties of closed-loop configurations can be used to correlate electromagnetic fields with carrier frequency differences beyond the GHz regime. Moreover, coherent control based on the relative phase in closed-loop configuration has been proposed in the context of quantum information processing [18].

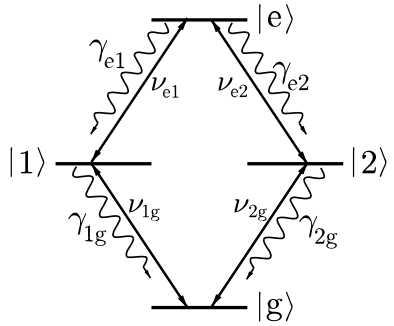

FIG. 1: Electronic transitions of the ♢-configuration. Each transition $|i\rangle \to |j\rangle$ is resonantly driven by a laser field at frequency ν_{ij}. Here, $|g\rangle$ is the ground state, $|1\rangle$ and $|2\rangle$ the intermediate states, which decay into the ground state at rates γ_{1g} and γ_{2g}, respectively, and $|e\rangle$ the excited state, which decays with rates γ_{e1} and γ_{e2} into the corresponding intermediate states. Each pair of levels is coupled by two paths of excitation, hence the dynamics depends critically on the relative phase between the paths. The coherent dynamics of this configuration is equivalent to the double-Λ scheme, while relevant differences with it originates from radiative decay.

In this work we investigate the phase-dependent dynamics of light propagation in a medium of atoms whose electronic levels are driven in a closed-loop configuration, denoted by the ♢ (diamond) scheme and sketched in Fig. 1. This configuration consists of four driven transitions where one ground state is coupled in a V-type structure to two intermediate states, which are in turn coupled to a common excited state in a Λ-type structure. It can be encountered, for instance, in (suitably driven) isotopes of alkali-earth atoms with zero nuclear spin [19]. Although the coherent dynamics of ♢ schemes is equivalent to that of double-Λ systems [7], the steady states of the two systems exhibit relevant differences due to the different relaxation processes [9, 10].

The dynamics of light propagation in a medium of ♢-atoms is studied by integrating numerically the Maxwell-Bloch equations. We find that, depending on the input field parameters, the polarization along the medium can be drastically modified. The propagation dynamics may exhibit two meta-stable values of the relative phase, namely the values 0 and π, corresponding to a semi-transparent and to an opaque medium, respectively. For different values of the initial phase, light propagation along the medium tends to one of these two values, depending on the input values of the driving amplitudes. These two types of metastable response are supported by the formation of atomic coherences leading to a minimization of dissipation by depleting the population of one or more atomic states. This metastable behavior is novel, to our knowledge, and offers promising perspectives in control techniques in quantum electronics.

The article is organized as follows. In Sec. II the model is introduced and discussed. In Sec. III the results for the dynamics of light propagation are reported and discussed in some parameter regimes. Conclusions and outlooks are reported in Sec. IV. The appendices present in detail equations and calculations at the basis of the model derived in Sec. II.

II. THE MODEL

We consider a classical field propagating in a dilute atomic gas along the positive z-direction. The field is composed by four optical frequencies ν_{1g}, ν_{2g}, ν_{e1} and ν_{e2}, its complex amplitude is a function of time t and position z of the form

$$\mathbf{E}(z,t)=\frac{1}{2}\sum_{i,j}\mathcal{E}_{ij}(z,t)\mathbf{e_{ij}}\mathrm{e}^{-i(\nu_{ij}t-k_{ij}z+\phi_{ij}(z,t))}+\text{c.c.}, \tag{1}$$

where we have denoted by k_{ij} and $\mathbf{e_{ij}}$ the wave vector and polarization of the frequency component ν_{ij}. The input field enters the medium at $z=0$, and the effect of coupling to the medium is accounted for in the z dependence of the amplitude $\mathcal{E}_{ij}(z,t)$ and phase $\phi_{ij}(z,t)$ whose variations in position and time are slow with respect to the wavelengths $\lambda_{ij}=2\pi/k_{ij}$ and the oscillation periods $T=2\pi/\nu_{ij}$, respectively. The atomic gas is very dilute and we can assume that the atoms interact with the fields individually. In particular, each field component at frequency ν_{ij} drives (quasi-) resonantly the electronic transition $|i\rangle\rightarrow|j\rangle$ of the atoms in the medium, such that the atomic levels are coupled in a ♢-shaped configuration.

The relevant atomic transitions and the coupling due to the lasers are displayed in Fig. 1. Here, $|g\rangle$ is the ground state, coupled by dipole transitions to the intermediate states $|1\rangle$, $|2\rangle$ at the dipole moments $\mathbf{d_{1g}}=\langle 1|\mathbf{d}|g\rangle$, $\mathbf{d_{2g}}=\langle 2|\mathbf{d}|g\rangle$, frequencies ω_1, ω_2, and decay rates γ_{1g} and γ_{2g}, respectively, to state $|g\rangle$. The intermediate states are also coupled to the excited state $|e\rangle$, at frequency ω_e with respect to the state $|g\rangle$, by the dipole transitions $\mathbf{d_{e1}}=\langle e|\mathbf{d}|1\rangle$, $\mathbf{d_{e2}}=\langle e|\mathbf{d}|2\rangle$. The excited state $|e\rangle$ decays into states $|1\rangle$ and $|2\rangle$ at rates γ_{e1} and γ_{e2}, respectively. A similar configuration of levels can be found in isotopes of alkali atoms with zero nuclear spin [19]. The dipole operator for the reduced Hilbert space of the electronic states of the atom is given by

$$\hat{\mathbf{d}}=\sum_{j=1,2}\left(\mathbf{d_{ej}}|j\rangle\langle e|+\mathbf{d_{jg}}|g\rangle\langle j|\right)+\text{H.c.}$$

Below we introduce the equations for field propagation and atomic dynamics, and make some preliminary considerations about the system.

A. Equations for field propagation

We denote by $\mathbf{P}(z,t)$ the macroscopic polarization

$$\mathbf{P}(z,t)=n\,\mathrm{Tr}\{\hat{\mathbf{d}}\sigma(z;t)\} \tag{2}$$

where $\hat{\mathbf{d}}$ is the dipole operator, n is the density of the medium, which we assume to be zero for $z<0$ and uniform for $z>0$, and $\sigma(z,t)$ is the atomic density matrix at time t and position z, which has been obtained by tracing out the other external degrees of freedom. Details of the underlying assumptions at the basis of Eq. (2) are discussed in Appendix A.

We decompose polarization $\mathbf{P}(z,t)$ into slowly- and fast-varying components, namely

$$\mathbf{P}(z,t)=\frac{1}{2}\sum_{i,j}\mathcal{P}_{ij}(z,t)\mathbf{e_{ij}}\mathrm{e}^{-i(\nu_{ij}t-k_{ij}z+\phi_{ij}(z,t))}+\text{c.c.}, \tag{3}$$

whereby the complex amplitudes $\mathcal{P}_{ij}$ and the phases ϕ_{ij} vary slowly as a function of position and time, and we consider the parameter regime where the driving fields are sufficiently weak, so that the generation of higher-order harmonics can be neglected. By comparison of Eqs. (2) and (3), the amplitudes $\mathcal{P}_{ij}$ can be expressed in terms of the elements of the density matrix σ,

$$\mathcal{P}_{ij}=2n\mathcal{D}_{ij}\sigma_{ij}e^{i(\nu_{ij}t-k_{ij}z+\chi_{ij})} \tag{4}$$

where $\sigma_{ij}=\langle i|\sigma|j\rangle$ and we have used $\mathbf{e_{ij}}\cdot\mathbf{d_{ji}}=\mathcal{D}_{ij}\mathrm{e}^{-\mathrm{i}\theta_{ij}}$, thereby separating the complex amplitudes $\mathcal{P}_{ij}$ into modulus and phase. Here, the term $\mathcal{D}_{ij}$ is real, θ_{ij} are the dipole phases ($\theta_{ij}=-\theta_{ji}$), and

$$\chi_{ij}(z,t)=\phi_{ij}(z,t)-\theta_{ij} \tag{5}$$

is the sum of the slowly-varying field phases $\phi_{ij}(z,t)$ and the dipole phases θ_{ij}.

Using definitions (1) and (3) and applying a coarse-grained description in time and space, the Maxwell equations simplify to a set of propagation equations for each

of the slowly-varying components of the laser and polarization fields [20]

$$\frac{\partial \mathcal{E}_{ij}}{\partial z} + \frac{1}{c}\frac{\partial \mathcal{E}_{ij}}{\partial t} = -\frac{\nu_{ij}}{2\,\epsilon_0\,c}\mathrm{Im}\{\mathcal{P}_{ij}(\mathcal{E}_{kl},\phi_{kl})\} \quad (6)$$

$$\frac{\partial \phi_{ij}}{\partial z} + \frac{1}{c}\frac{\partial \phi_{ij}}{\partial t} = -\frac{\nu_{ij}}{2\,\epsilon_0\,c}\frac{1}{\mathcal{E}_{ij}}\mathrm{Re}\{\mathcal{P}_{ij}(\mathcal{E}_{kl},\phi_{kl})\}. \quad (7)$$

which are defined for $z > 0$. Here, each amplitude $\mathcal{E}_{ij}$ of the laser field component at frequency ν_{ij} is coupled via the polarization components $\mathcal{P}_{ij}$ to the other field components at amplitudes $\mathcal{E}_{kl}$ and phases ϕ_{kl}.

We rescale the propagation equations using the dimensionless length $\xi = \kappa_{1g} z$ and dimensionless time $\tau = c\,\kappa_{1g} t$, where κ_{1g} is the absorption coefficient

$$\kappa_{1g} = n\frac{1}{\gamma_{1g}}\frac{\nu_{1g}\mathcal{D}_{1g}^2}{c\epsilon_0\hbar} \quad (8)$$

such that $1/\kappa_{1g}$ determines the characteristic length at which light penetrates a medium of dipoles at density n, transition frequency ν_{1g} and linewidth γ_{1g}. We denote the dimensionless field amplitudes by

$$\mathcal{G}_{ij} = \frac{\Omega_{ij}}{\gamma_{1g}}\frac{\mathcal{D}_{1g}^2\nu_{1g}}{\mathcal{D}_{ij}^2\nu_{ij}}, \quad (9)$$

where

$$\Omega_{ij}(z,t) = \mathcal{D}_{ij}\mathcal{E}_{ij}(z,t)/\hbar \quad (10)$$

is the real valued Rabi frequency for the transition $|i\rangle \to |j\rangle$. With this notation Eqs. (6) and (7) reduce to the form

$$\frac{\partial \mathcal{G}_{ij}}{\partial \xi} + \frac{\partial \mathcal{G}_{ij}}{\partial \tau} = -\,\mathrm{Im}\{p_{ij}\} \quad (11)$$

$$\frac{\partial \phi_{ij}}{\partial \xi} + \frac{\partial \phi_{ij}}{\partial \tau} = -\,\frac{1}{\mathcal{G}_{ij}}\,\mathrm{Re}\{p_{ij}\}, \quad (12)$$

where

$$p_{ij}(\xi,\tau) = \sigma_{ij}\mathrm{exp}\left[i\left(\frac{\nu_{ij}}{c\,\kappa_{1g}}\tau - \frac{k_{ij}}{\kappa_{1g}}\xi + \chi_{ij})\right)\right]. \quad (13)$$

In the remainder of this paper we consider laser field geometries where $|1\rangle$ and $|2\rangle$ are states of the same hyperfine multiplet so that $\nu_{1g} \simeq \nu_{2g}$ and $\nu_{e1} \simeq \nu_{e2}$.

B. Atomic dynamics

The time evolution of the density matrix $\sigma(z,t)$ for the atomic internal degrees of freedom at position $z > 0$ is governed by the master equation

$$\dot{\sigma} = \frac{1}{\mathrm{i}\hbar}\,[H(z,t),\sigma] + \mathcal{L}\sigma. \quad (14)$$

where z is a classical variable. Equation (14) is obtained by tracing out the degrees of freedom of momentum and of position in the transverse plane, in the limit in which the medium is homogeneously broadened and the atoms are sufficiently hot and dilute such that their external degrees of freedom can be treated classically. Details of the assumptions at the basis of Eq. (14) are reported in Appendix A. Here the Hamiltonian

$$\begin{aligned} H(z,t) \;=\; & \sum_{j=e,1,2,g}\hbar\omega_j|j\rangle\langle j| \quad (15)\\ & -\;\frac{\hbar}{2}\sum_{j=1,2}\Big(\Omega_{jg}(z,t)\;e^{-i(\nu_{jg}t-k_{jg}z+\chi_{jg}(z,t))}\;|j\rangle\langle g| \\ & \quad +\Omega_{ej}(z,t)\;e^{-i(\nu_{ej}t-k_{ej}z+\chi_{ej}(z,t))}\;|e\rangle\langle j| + \mathrm{H.c.}\Big) \end{aligned}$$

describes the coherent dynamics of the internal degrees of freedom, and it depends on z through the (real-valued) Rabi frequency, Eq. (10), and through the corresponding phase of field and dipole.

The states $|1\rangle, |2\rangle, |e\rangle$ are unstable and decay radiatively with rates γ_{1g}, γ_{2g}, γ_e, respectively. The relaxation processes are described by

$$\begin{aligned} \mathcal{L}\sigma \;=\; & \sum_{j=1,2}\frac{\gamma_{jg}}{2}\,(2|g\rangle\langle j|\sigma|j\rangle\langle g| - |j\rangle\langle j|\sigma - \sigma|j\rangle\langle j|) \quad (16)\\ & +\;\sum_{j=1,2}\frac{\gamma_{ej}}{2}\,(2|j\rangle\langle e|\sigma|e\rangle\langle j| - |e\rangle\langle e|\sigma - \sigma|e\rangle\langle e|) \end{aligned}$$

where $\gamma_{e1}+\gamma_{e2} = \gamma_e$. In this paper we assume $\gamma_{ej} = \gamma_e/2$. We remark that in Eq. (16) the recoil due to spontaneous emission is neglected since the motion is considered classical. Note that the transitions $|g\rangle \to |j\rangle$ $(j = 1, 2)$ are saturated when $\Omega_{jg} \geq \gamma_{jg}$. Correspondingly, the upper transitions $|j\rangle \to |e\rangle$ are saturated when $\Omega_{ej} \geq \gamma_e + \gamma_{jg}$. For later convenience, we introduce

$$\tilde{\mathcal{G}}_{ej} = \frac{\mathcal{G}_{ej}}{1+\gamma_e/\gamma_{jg}},$$

which explicitly shows the scalings of the upper fields amplitudes with the corresponding dissipation rates.

C. The relative phase

In the so-called *closed-loop* configurations, like in the $\diamondsuit$ scheme, transitions between each pair of electronic levels are characterized by -at least- two excitation paths, involving different intermediate atomic levels [8, 11]. In the $\diamondsuit$ scheme the relative phase

$$\Delta\chi(z,t) = \chi_{e1}(z,t)+\chi_{1g}(z,t)-\chi_{e2}(z,t)-\chi_{2g}(z,t) \quad (17)$$

with χ_{ij} defined in Eq. (5), critically determines the solution of the master equation, and hence atomic response to propagation. The role of the relative phase (17) in the atomic response is better unveiled by moving to a suitable reference frame for the atomic evolution, which is defined when all amplitudes $\mathcal{E}_{ij}$ are nonzero. We denote

by ρ the density matrix in this reference frame, obeying the master equation

$$\dot{\rho} = \frac{1}{i\hbar}\left[\tilde{H}, \rho\right] + \mathcal{L}\rho. \tag{18}$$

Here the transformed Hamiltonian $\tilde{H}$ reads [7, 10]

$$\begin{aligned}\tilde{H} &= \hbar\Delta_e|e\rangle\langle e| + \hbar\Delta_1|1\rangle\langle 1| + \hbar\Delta_2|2\rangle\langle 2| \\ &- \frac{\hbar}{2}\Big(\Omega_{e1}\,|e\rangle\langle 1| + \Omega_{e2}\,\mathrm{e}^{\mathrm{i}\Theta(t,z)}\,|e\rangle\langle 2| \\ &+\Omega_{1g}\,|1\rangle\langle g| + \Omega_{2g}\,|2\rangle\langle g| + \mathrm{H.c.}\Big)\,,\end{aligned} \tag{19}$$

with the detunings

$$\Delta_1 = \omega_1 - \nu_{1g} \tag{20}$$
$$\Delta_2 = \omega_2 - \nu_{2g} \tag{21}$$
$$\Delta_e = \omega_e - \nu_{e1} - \nu_{1g}. \tag{22}$$

The Hamiltonian (19) exhibits an explicit dependence on the phase

$$\Theta(z,t) = \Delta\nu\; t - \Delta k\; z - \Delta\theta + \Delta\phi(z,t). \tag{23}$$

where

$$\Delta\nu = \nu_{e1} + \nu_{1g} - \nu_{2g} - \nu_{e2} \tag{24}$$
$$\Delta k = k_{e1} + k_{1g} - k_{2g} - k_{e2} \tag{25}$$
$$\Delta\theta = \theta_{e1} + \theta_{1g} - \theta_{2g} - \theta_{e2}. \tag{26}$$

The quantity $\Delta\nu$ is the four-photon detuning of the laser frequencies, Δk is the wave-vector mismatch and $\Delta\theta$ is the relative dipole phase. In [9, 10] it has been discussed how Θ affects the dynamics of the atom. In particular, when $\Delta\nu = 0$ a steady state exists and it is critically determined by the value of Θ, entering master equation (18) through the Hamiltonian (19). In the remainder of this article we assume

$$\Delta\nu = 0,\ \Delta k = 0,$$

namely the atoms are driven at four-photon resonance and by copropagating laser fields, such that the wave vector mismatch is negligible. Hence, the phase Θ depends solely on the relative dipole phase, which is constant, and on the relative phase of the propagating fields, which evolves according to the coupled Eqs. (11) and (12).

We use relations $\rho_{g1} = p_{g1}$, $\rho_{g2} = p_{g2}$, $\rho_{e1} = p_{e1}$, and

$$p_{e2} = \rho_{e2}\exp\left(\mathrm{i}\Theta\right),$$

which connect the elements of the density matrix ρ in the new reference frame with the elements p_{ij}. Substituting into Eqs. (11)-(12), we find

$$\frac{\partial\mathcal{G}_{jg}}{\partial\xi'} = -\mathrm{Im}\{\rho_{jg}\} \tag{27}$$
$$\frac{\partial\phi_{jg}}{\partial\xi'} = -\frac{\mathrm{Re}\{\rho_{jg}\}}{\mathcal{G}_{jg}}\,. \tag{28}$$

for $j = 1, 2$ and

$$\frac{\partial\mathcal{G}_{e1}}{\partial\xi'} = -\mathrm{Im}\{\rho_{e1}\} \tag{29}$$
$$\frac{\partial\phi_{e1}}{\partial\xi'} = -\frac{\mathrm{Re}\{\rho_{e1}\}}{\mathcal{G}_{e1}}. \tag{30}$$
$$\frac{\partial\mathcal{G}_{e2}}{\partial\xi'} = -\mathrm{Im}\{\rho_{e2}e^{i\Theta}\} \tag{31}$$
$$\frac{\partial\phi_{e2}}{\partial\xi'} = -\frac{\mathrm{Re}\{\rho_{e2}e^{i\Theta}\}}{\mathcal{G}_{e2}}. \tag{32}$$

where we have introduced the variable

$$\xi' = \xi + \tau.$$

We remark that the value of the terms ρ_{ij} depends on the amplitudes of the fields and on the value of the phase Θ, as it is visible from Eq. (18) and (19). The propagation dynamics now consist in solving the coupled equation (18) and Eqs. (27)-(32). The optical Bloch equations for the density matrix ρ are presented in Appendix B.

In general, the density matrix elements entering Eqs. (27)-(32) are time dependent, i.e., $\rho = \rho(\tau)$. In this paper we consider the case of sufficiently long laser pulses, such that the characteristic time of change of amplitude and phase of the fields and the interaction time between light and atoms exceed the time scale in which the atom reaches the internal steady state. In this regime, we can neglect transient effects, and the density matrix elements entering Eqs. (27)-(32) are the stationary solutions of Eq. (18) satisfying $\partial\rho/\partial t = 0$. This assumption allows us to neglect the time derivative in Eqs. (27)-(32), hence taking $\xi' \approx \xi$.

III. LIGHT PROPAGATION IN THE ♢-MEDIUM

In this section we study light propagation in a medium of ♢-atoms by solving numerically the Maxwell-Bloch Equations, Eqs. (18) and (27)-(32). We restrict ourselves to some parameter regimes, with the purpose of singling out the role played by the phase and the radiative decay processes in the dynamics. In particular, we consider the situation where each atomic transition is driven at resonance, namely

$$\Delta_i = 0,$$

for $i = 1, 2, e$. Moreover, we restrict to the regime where the fields are initially driving the corresponding transitions at saturation. This latter assumption is important to guarantee a finite occupation of the excited state $|e\rangle$, and thus to highlight the dependence of the dynamics on the relative phase Θ.

During the propagation dynamics, it may occur that one of the field amplitudes vanishes in just one point of the propagation variable ξ'. When this happens, the relative phase Θ is not defined and its value must be reset

manually to continue the propagation when integrating the field equations in amplitude and phase (see Eqs. (27)-(32)). In such cases the value of the chosen phase depends on the field amplitude that vanishes. The correctness of this procedure has been checked by comparing the results with those obtained by integrating the field equations for the real and imaginary parts of the complex fields amplitudes.

A. Symmetric drives

We consider the parameter regime such that the laser amplitudes driving the upper (lower) transitions are initially equal, namely

$$\mathcal{G}_{e1}(0) = \mathcal{G}_{e2}(0) = \mathcal{G}_e \tag{33}$$
$$\mathcal{G}_{1g}(0) = \mathcal{G}_{2g}(0) = \mathcal{G}_g. \tag{34}$$

For these input amplitudes the components of the polarizations entering the equations for the field phases, Eqs. (28), (30) and (32), and determining the evolution of the phase along the medium, vanish for $\Theta = \ell\pi$, with ℓ being an integer [10]. Hence, if at the input

$$\Theta(\xi = 0) = \ell\pi, \tag{35}$$

then

$$\frac{\partial\Theta}{\partial\xi} = 0 \tag{36}$$

and the relative phase remains constant during propagation along the medium. On the other hand, the components of the polarization in the equations for the field amplitude, determining how energy is dissipated along the medium, depend critically on whether ℓ in Eq. (35) is even or odd. Below we discuss these two cases in detail and comment on the phase stability during propagation.

1. *Light propagation for* $\Theta(0) = \pi$

For ℓ odd, say $\Theta(0) = \pi$, the polarizations of the transitions between the intermediate and the upper states identically vanish, i.e., $\rho_{e1} = \rho_{e2} = 0$ [10]. Therefore, the atoms are perfectly decoupled from the upper fields independently of their intensity. This is an interference effect arising from the fact that the upper transitions are driven in opposition of phase with respect to the lower transitions. As a consequence the excited state is not populated. It can be shown that in this regime the global atomic dynamics can be mapped onto the ones of two-level transitions where the ground state is coupled to a coherence between the intermediate states, that is an EIT-coherence for the upper fields [7, 10]. Correspondingly, the dynamics of light propagation of the lower fields is expected to be the one encountered in a medium of V-atoms.

Figure 2(a) displays the propagation dynamics along the medium when $\Theta(0) = \pi$ and $\mathcal{G}_{ij}(0) = \mathcal{G}_0$. Here, one sees that the upper fields propagate through the medium as if it were transparent, keeping a constant value $\mathcal{G}_{ej} = \mathcal{G}_0$. The amplitudes of the lower fields decay in the same way, i.e., $\mathcal{G}_{1g}(\xi) = \mathcal{G}_{2g}(\xi)$. Figure 2(b) displays the corresponding populations of the electronic levels along the medium. The electronic level $|e\rangle$ remains depleted and the intermediate states $|1\rangle$ and $|2\rangle$ are equally occupied as a function of ξ, corresponding to the fact that $\mathcal{G}_{1g}(\xi) = \mathcal{G}_{2g}(\xi)$ along the medium. The value of ground and intermediate state populations remains constant until about $\xi \sim 200$ till the fields $\mathcal{G}_{jg}(\xi)$ saturate the respective transitions, and they undergo a fast change when the lower field amplitudes drive the lower transitions below saturation so that only the ground state is appreciably occupied. Note that these dynamics are independent of the value of $\mathcal{G}_{e1}, \mathcal{G}_{e2}$, as these fields remain decoupled from the atoms.

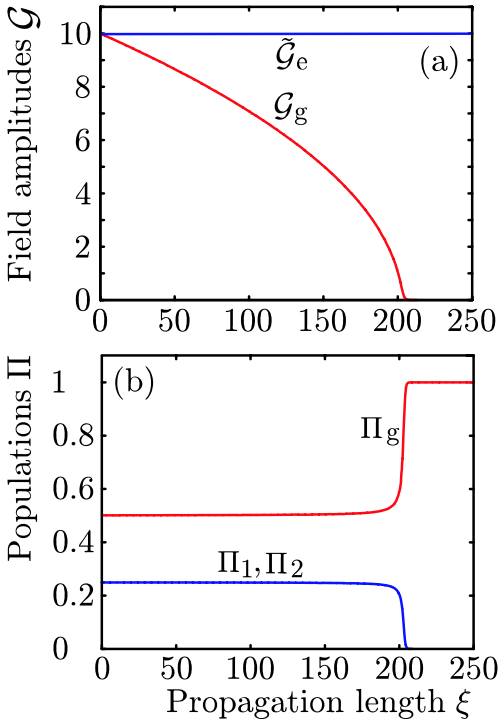

FIG. 2: (color online) (a) Rescaled field amplitudes $\mathcal{G}_g$ and $\tilde{\mathcal{G}}_e$ as a function of the propagation length ξ for $\mathcal{G}_g(0) = \tilde{\mathcal{G}}_e(0) = 10$ and $\Theta(0) = \pi$. The behaviour is independent of the value of γ_e and of $\tilde{\mathcal{G}}_e$, and the upper fields propagate unperturbed through the medium. (b) Populations of the electronic levels $\Pi_i = \langle i|\rho|i\rangle$ as a function of the propagation length. The excited state $|e\rangle$ remains depleted along the medium.

The dynamics described in Fig. 2 is also apparent when we inspect the propagation equations for $\Theta(0) = \pi$. Setting $\mathcal{G}_{e1}(0) = \mathcal{G}_{e2}(0) = \mathcal{G}_e$ and $\mathcal{G}_{1g}(0) = \mathcal{G}_{2g}(0) = \mathcal{G}_g$, we obtain, together with Eq. (36), the equations for the

dimensionless amplitudes

$$\frac{\partial \mathcal{G}_g}{\partial \xi} = -\frac{\mathcal{G}_g}{1+4\mathcal{G}_g^2}, \tag{37}$$

$$\frac{\partial \mathcal{G}_e}{\partial \xi} = 0, \tag{38}$$

where Eq. (38) vanishes since $\mathrm{Im}\{\rho_{ij}(\Theta = \pi)\} = 0$. Therefore, the relative phase Θ and the upper field amplitudes $\mathcal{G}_e$ are constant along the medium and the medium is transparent to the upper fields. In particular, the propagation of the amplitudes $\mathcal{G}_g$ depends only on the value of $\mathcal{G}_g$ itself, and Eq. (37) has the same form of the equations of an electric field propagating in a medium of resonant dipoles. Numerical investigations show that this dynamics at $\Theta = \pi$ is robust against phase and amplitudes fluctuations, showing that this type of response of the medium is a metastable configuration. It should be remarked that this behavior is transient, since the medium dissipates the lower fields until the atoms are all found in the ground state well inside the medium. Nevertheless, even when the intermediate states are appreciably occupied, the upper fields propagate through the medium as if it were transparent.

2. *Light propagation for* $\Theta(0) = 0$

When $\Theta = 0$, two photon processes are characterized by paths of excitations which can interfere constructively. In this regime, atomic coherences between either the intermediates states or the ground and excited states may form, and correspondingly the imaginary part of the polarizations may become very small, thus reducing dissipation. The appearance of this dynamics is critically determined by the ratio between the decay rate of the intermediate states and that of the excited state, namely on the parameter

$$\alpha = \frac{\gamma_e}{\gamma_{1g} + \gamma_{2g}}. \tag{39}$$

In [10] we showed that when this ratio is appreciably different from unity and $\Theta = 0$, metastable EIT-coherences [1] characterize the atomic steady state. We now investigate how light propagates for different values of α when the phase is initially set to the value $\Theta(0) = 0$.

We first consider the propagation equations setting initially $\Theta(0) = 0$, $\tilde{\mathcal{G}}_{e1}(0) = \tilde{\mathcal{G}}_{e2}(0) = \tilde{\mathcal{G}}_e(0)$ and $\mathcal{G}_{1g}(0) = \mathcal{G}_{2g}(0) = \mathcal{G}_g(0)$. Figure 3 displays the propagation dynamics along the medium for different values of the ratio α. For $\alpha \gg 1$ and $\alpha \ll 1$ the amplitudes decay slowly as a function of ξ, as expected from the formation of EIT-coherences. In [10] it has been shown that these coherences may originate population inversion at steady state. In particular, for $\alpha \ll 1$ and $\Theta = 0$ the atom can exhibit population inversion between the excited and the

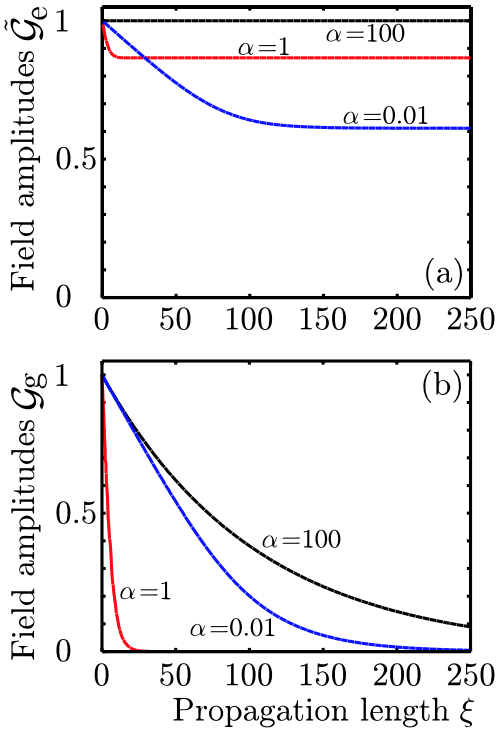

FIG. 3: (color online) Rescaled field amplitudes (a) $\tilde{\mathcal{G}}_e$ and (b) $\mathcal{G}_g$ as a function of the propagation length ξ for $\Theta(0) = 0$, $\tilde{\mathcal{G}}_e(0) = \mathcal{G}_g(0) = 1$ and $\alpha = 100$ (black), $\alpha = 1$ (red), and $\alpha = 0.01$ (blue).

intermediate states at the steady state for some parameter regimes. Similarly, for $\alpha \gg 1$ population inversion at steady state was observed between the intermediate and the ground states. Figure 4 shows light propagation, when the initial conditions over the fields give population inversion at steady state. Here, one sees that population inversion is found also along the absorbing medium and it gradually decreases since the atomic coherences are metastable.

In the simulations of Figures 3 and 4, the lower (upper) field amplitudes remain equal to one another during propagation. If we assume that $\mathcal{G}_{e1} = \mathcal{G}_{e2} = \mathcal{G}_e$ and $\mathcal{G}_{1g} = \mathcal{G}_{2g} = \mathcal{G}_g$ for all relevant ξ, then the propagation equations for the amplitudes reduce to the equations for $\mathcal{G}_e(\xi)$ and $\mathcal{G}_g(\xi)$ with the form

$$\frac{\partial \mathcal{G}_e}{\partial \xi} = -\frac{\mathcal{G}_e\, \mathcal{G}_g^2\, \alpha}{D_0}\,(1+2\alpha), \tag{40}$$

$$\frac{\partial \mathcal{G}_g}{\partial \xi} = -\frac{\mathcal{G}_g\, \alpha}{D_0}\,\left[\mathcal{G}_g^2 + \alpha + 2\alpha^2 + \mathcal{G}_e^2\,(1+\alpha)\right], \tag{41}$$

with

$$\begin{aligned} D_0 \;=\; & \mathcal{G}_e^4\,(1+\alpha) + (1+4\mathcal{G}_g^2)\,\alpha\,(\mathcal{G}_g^2 + \alpha + 2\alpha^2) \\ & + \mathcal{G}_e^2\,\left[\alpha\,(2+3\alpha) + \mathcal{G}_g^2\,(1+3\alpha+2\alpha^2)\right]. \end{aligned} \tag{42}$$

Equations (40) and (41) describe the dissipative propagation of the field amplitudes, and exhibit a nonlinear

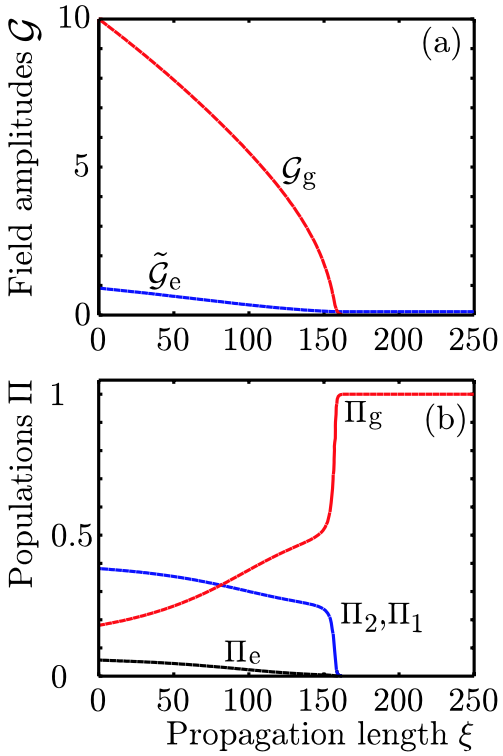

FIG. 4: (color online) (a) Field amplitudes $\tilde{\mathcal{G}}_e$ (blue) and $\mathcal{G}_g$ (red) as a function of the propagation length ξ for $\tilde{\mathcal{G}}_e(0) = 1$, $\mathcal{G}_g(0) = 10$, $\alpha = 10$ and $\Theta(0) = 0$. (b) Population of the electronic levels Π_g (red), Π_1, Π_2 (blue) and Π_e (black). Population inversion between the intermediate levels and the ground level is seen along the medium until $\xi \approx 80$.

dependence on the amplitudes and the ratio α of the decay constants. Here, one can see that for different values of α the absorption lengths can vary by orders of magnitude. Limit cases are found when $\alpha \to 0$, i.e. when the excited state is stable, and $\alpha \to \infty$, i.e. when the intermediate states are stable. In these cases, the right hand sides of Eqs. (40) and (41) vanish, damping is absent, and light propagates through the medium as if it was transparent [21].

In the cases discussed so far, energy is exchanged between upper and lower fields until the lower fields amplitudes are damped below saturation. Then, the upper fields decouple as the population of the intermediate states is negligible. In order to study the long term dynamics of propagation, we now focus onto the regime where the lower transitions are driven very well above saturation and where we expect different length scales for the propagation of the upper and lower fields.

Figure 5 displays propagation when initially $\mathcal{G}_g(0) = 10$ and $\tilde{\mathcal{G}}_e(0) = 1$, for different values of α. We discuss case by case, starting from the case of $\alpha = 1$ where upper and lower transitions dissipate at comparable rates. The dynamics observed in the $\alpha = 1$ case clearly separates the regimes corresponding to $\alpha = 0.01$ and $\alpha = 100$.

Case $\alpha = 1$. In Fig. 5(c) the amplitudes of the fields decay steadily along the medium. Correspondingly, the behavior of the population is shown in Fig. 5(d). Here, one sees that when the Rabi frequency is larger than the saturation value, the population of the ground and intermediate states are different from zero and constant, while the excited state is nearly depleted. When the lower field amplitudes are damped below saturation, the ground state population increases while the intermediate states populations accordingly vanish.

Case $\alpha = 100$. In Fig. 5(a) the decay of the lower field amplitudes $\mathcal{G}_g$ differ strikingly from the behavior usually encountered in a medium of dipoles. Moreover, the upper field amplitudes $\mathcal{G}_e$ remain almost constant along the medium. Further insight into the dynamics can be gained by analyzing the corresponding atomic state populations. In Fig. 5(b) the excited state is nearly depleted, the intermediate states are initially as populated as the ground state, and their population decrease gradually during propagation. From further analysis one can infer that atomic coherence between states $|1\rangle$ and $|2\rangle$ characterizes the propagation dynamics of the upper fields which thus decouple from the excited state $|e\rangle$ due to destructive interference in a way similar to the response of EIT-media. In this case, this atomic coherence is unstable due to decay of the intermediate states. It is established through the medium by the action of the lower fields that pump atoms into the upper states as long as they drive the lower transitions well above saturation, and by the faster decay of the excited state capable to create transient coherences. The formation of these coherences have been observed in the transient dynamics of pulse propagation in a medium of $\diamondsuit$-atoms [13]. Differently from the case discussed in Fig. 4, the parameter regime here does not support population inversion, and the intermediate states are initially almost as populated as the ground state.

Case $\alpha = 0.01$. An entirely different behavior is encountered for $\alpha = 0.01$. In Fig. 5(e) the upper fields amplitudes, initially equal to each other, become different during propagation so that after a certain propagation length one increases, $\tilde{\mathcal{G}}_{e1}$, while the other, $\tilde{\mathcal{G}}_{e2}$, decreases until it vanishes. At this point, the relative phase Θ jumps from zero to π, $\tilde{\mathcal{G}}_{e2}$ starts to increase again while $\tilde{\mathcal{G}}_{e1}$ keeps decreasing till they reach almost the same value. After this transient, the field amplitudes of the excited states maintain a constant value across the medium. Correspondingly, during and after this transient, the excited state population in Fig. 5(f) decreases until it reaches zero. This remarkable behavior hints to an instability of the phase value $\Theta = 0$, which seems to be triggered here by numerical fluctuations of the values of the upper field amplitudes. This conjecture is supported by the numerical analysis shown in Fig. 6 and where the initial values of the upper field amplitudes vary of (a) one part over 10^{-16}, (b) one part over 10^{-12} and (c) one part over 10^{-8}. As the initial discrepancy increases, this behavior appears at earlier locations in the medium. Investigations on populations and phases show that the

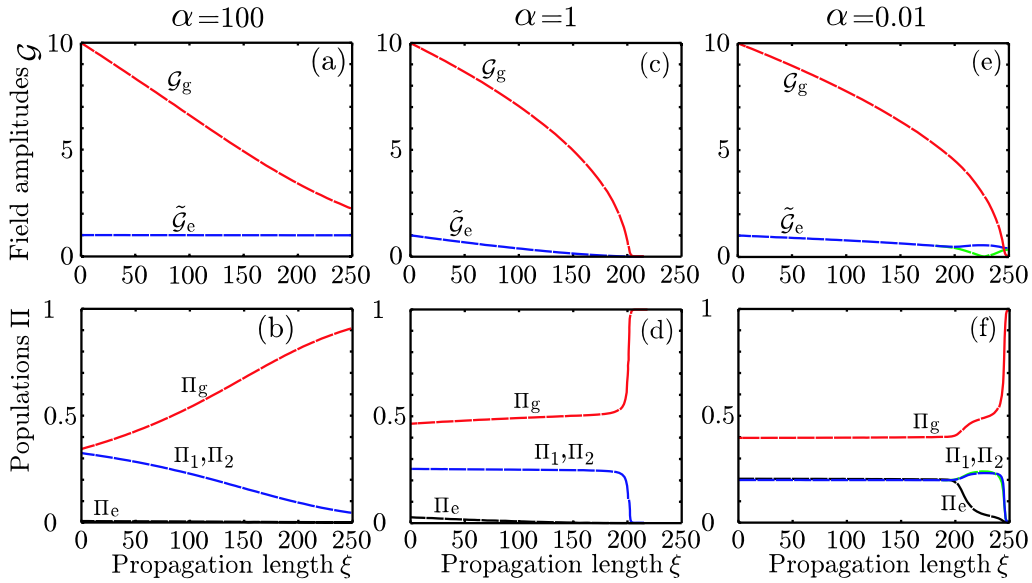

FIG. 5: (color online) Upper row: Field amplitudes $\tilde{\mathcal{G}}_e$ (blue) and $\mathcal{G}_g$ (red) as a function of the propagation length ξ, for $\Theta(0) = 0$, $\mathcal{G}_g(0) = 10$ and $\tilde{\mathcal{G}}_e(0) = 1$. Lower row: Corresponding populations of the electronic levels Π_g (red), Π_1, Π_2(blue), and Π_e (black), as a function of the propagation length. Here, (a) and (b) correspond to the case $\alpha = 100$, (c) and (d) to the case $\alpha = 1$, and (e) and (f) to the case $\alpha = 0.01$.

unbalance between the upper field amplitudes induces a depletion of the excited state until the vanishing of one of the upper amplitudes forces a phase jump to the value $\Theta = \pi$ and the system settles to the situation where the upper fields decouple from the atom. After the phase jump, the upper field amplitudes tend to recover an equal value, but they end to decouple from the atom once the lower field amplitudes have vanished.

The phase $\Theta = 0$ is hence unstable and its instability is driven by small fluctuations in the difference of the initial field amplitudes. Such instability, however, moves to further propagation lengths as α increases, i.e. when the decay rate of the excited state increases. This case is investigated in Fig. 7, where one can see that the symmetry breaking is progressively delayed and finally moves to distances where all fields have been completely absorbed by the medium, as the value of α varies from 0.001 to 0.1 and for the same initial difference between the two upper field values of one part over 10^{-8}.

The behavior described in Fig. 7 is due to the long term occupation of the excited state. In particular, for $\Theta = 0$ and $\alpha \ll 1$ the excited state is very stable and a long term coherence is built between the ground and excited states. Such coherence is similar to that encountered in a cascade, Ξ, configuration [22] and indeed for $\Theta = 0$ and symmetric drives the $\diamondsuit$-level system can be mapped onto a Ξ scheme [7, 10]. However, such dynamics is unstable since small differences of the upper field amplitudes lead to a phase jump and to the depletion of the excited state. In the new configuration the upper fields decouple from the intermediate states by means of a different atomic coherence effect. In fact in the regime corresponding to $\Theta = \pi$, the intermediate levels get appreciably occupied while the dynamics of propagation becomes unaffected by the upper fields. In this regime, the dynamics of the $\diamondsuit$-level system can be mapped onto the one of a V-level scheme [10]. This behavior may appear contradictory since the upper fields are now expected to populate the excited state by depleting the intermediate ones. However, for $\Theta = \pi$, CPT takes place in the upper Λ of the $\diamondsuit$ system, the intermediate states become decoupled from the excited state and the upper fields are not absorbed. We then explain the phase jump from $\Theta = 0$ to $\Theta = \pi$ as the tendency for the system to minimize the rate of dissipation. This behavior is reminiscent of the dynamics observed in Four-Wave Mixing experiments where interference effects are generated in order to minimize spontaneous emission [23].

3. *Light propagation for a generic initial phase*

In this section we discuss light propagation for input parameters (33) and (34) and phase $\Theta \neq \ell\pi$. In particular, we choose $\Theta(0) = \pi/2$, as for the numerical studies made for other values of the phase $\Theta \neq \ell\pi$ the dynamics does not change substantially, so that this case can be considered exemplary.

Figures 8 and 9 display the amplitude and the relative phase of the propagating fields for $\alpha = 0.01, 100$. Although the field amplitudes are clearly damped for all values of α, the mechanism of radiation dissipation depends on α and on the initial strengths of the field amplitudes. We can identify two behaviors of the dynamics of propagation depending on how strongly the lower fields saturate the corresponding transitions.

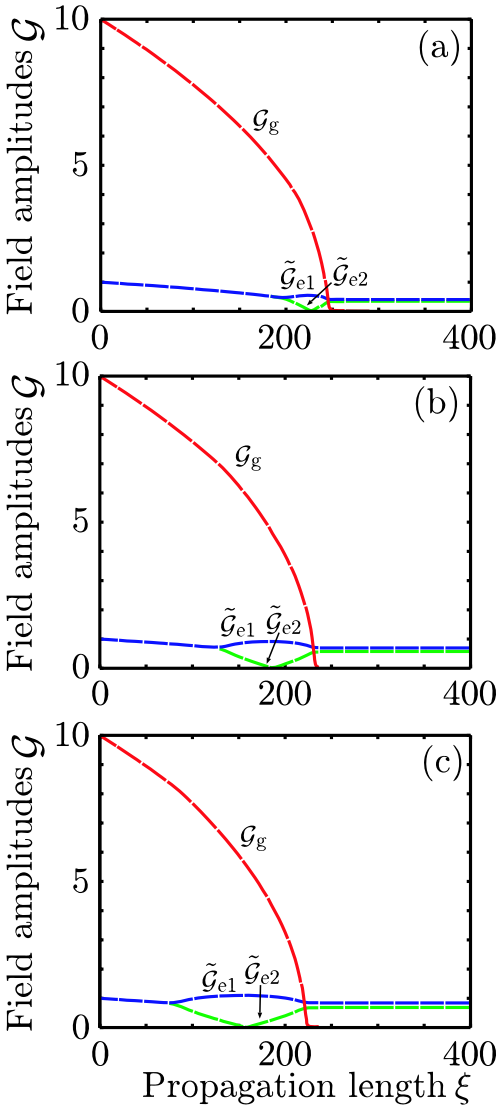

FIG. 6: (color online) Field amplitudes $\mathcal{G}_g$ (red), $\tilde{\mathcal{G}}_{e1}$ (blue) and $\tilde{\mathcal{G}}_{e2}$ (green) as a function or the propagation length ξ, for $\alpha = 0.01$, $\mathcal{G}_{1g}(0) = \mathcal{G}_{2g}(0) = \mathcal{G}_g = 10$, $\tilde{\mathcal{G}}_{e1}(0) = 1$ and (a) $\tilde{\mathcal{G}}_{e2}(0) = \mathcal{G}_{e1}(0)$, (b)$\tilde{\mathcal{G}}_{e2}(0) = \tilde{\mathcal{G}}_{e1}(0) - 10^{-12}$ and (c)$\tilde{\mathcal{G}}_{e2}(0) = \tilde{\mathcal{G}}_{e1}(0) - 10^{-8}$.

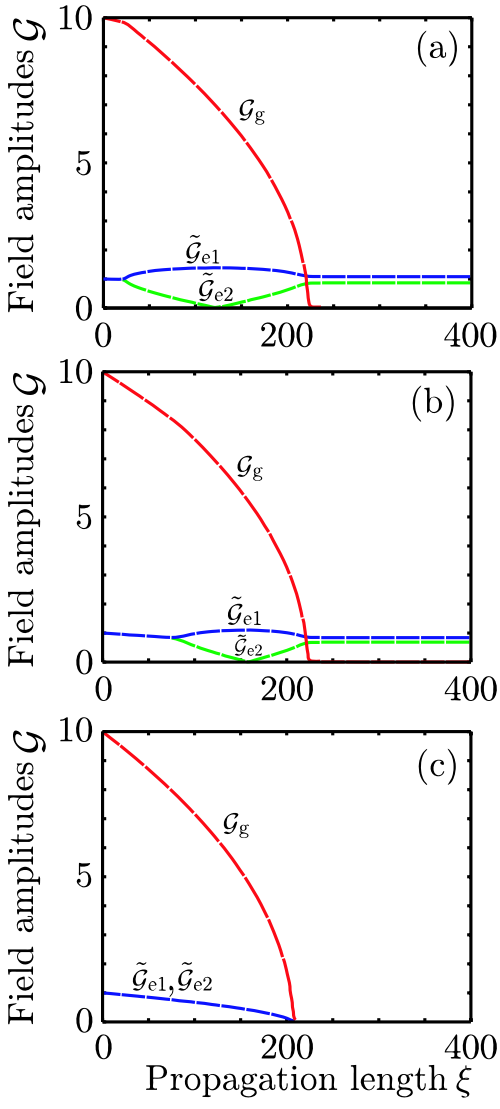

FIG. 7: (color online) Field amplitudes $\mathcal{G}_g$ (red), $\tilde{\mathcal{G}}_{e1}$ (blue) and $\tilde{\mathcal{G}}_{e2}$ (green) as a function of the propagation length ξ, for $\mathcal{G}_{g1}(0) = \mathcal{G}_{g2}(0) = \mathcal{G}_g(0) = 10$, $\mathcal{G}_{e1}(0) = 1$, $\mathcal{G}_{e2}(0) = \mathcal{G}_{e1}(0) - 10^{-8}$ and (a) $\alpha = 0.001$, (b) $\alpha = 0.01$ and (c) $\alpha = 0.1$.

In Figure 8 the saturation parameters in the upper transition is larger or equal to the saturation parameters in the lower transitions. Here, we observe that the phase of the field tends to the zero value. Before this value is reached, radiation is damped at a fast rate. Once the value $\Theta = 0$ is reached, the slope of the lower-amplitude curves changes abruptly and decays more slowly. This sudden change in the behavior occurs at a propagation length determined by the typical absorption length of the fast decaying transition. The system tends to configurations corresponding to $\Theta = 0$, thereby switching to an EIT-like response. A similar kind of behavior is also observed in a medium of the Double-Λ atoms where EIT-coherences are established between the two stable states [9]. In the $\diamondsuit$ configuration, the atomic coherences that characterize the dynamics when the phase reaches the value $\Theta = 0$ are also EIT-like, whereby due to the coherence instability the interference phenomenon is transient [14]. Depending on the value of α, coherences are established either between the intermediate states, like in a Λ configuration, or between the ground and excited states, like in a Ξ configuration. This latter case is encountered for $\alpha = 0.01$, and leads to population inversion between the excited and the intermediate states along the medium, see Fig. 8(f), whereby the population of the intermediate states gets very small.

Figure 9 displays the situation, when the lower transitions are driven well above saturation, and the corresponding saturation parameter is larger than the saturation parameter for the upper fields. Here, the phase

slowly tends to the value π where the upper transitions are decoupled from the fields. In this case, the typical propagation length at which the π value of the phase is reached is larger than in the previous cases. Nonetheless, the tendency of the medium is to reach the situation in which the upper fields are decoupled. This kind of behavior corresponds to the creation of a coherence between the intermediate states which is decoupled from the upper fields since it is out of phase with respect to these drives. The onset of this dynamics depends critically on the value of $\mathcal{G}_g$. The field amplitudes must well saturate the lower transitions with respect to $\mathcal{G}_e$ so to populate the intermediate states on a time scale shorter than their decay rate, but long enough for incoherent decay of the upper state to take place. This behavior is in agreement with the observation of the instability of the phase $\Theta = 0$ when the lower transitions are driven well above saturation, showing that for this parameter regime the value $\Theta = \pi$ is the stable one.

B. Four-wave mixing

In this section we discuss propagation when one field is initially very weak while the other three transitions are driven at saturation. Figures 10 and 11 display the fields propagation when the upper field amplitude $\mathcal{G}_{e2}$ is very small and the phase is initially set to the value $\Theta(0) = \pi/2$. In both cases one observes amplification of the weak field. In the case displayed in Fig. 10 amplification is accompanied by the asymptotic approach to the value $\Theta = \pi$ while in the case of Fig. 11 to the value $\Theta = 0$. Let us now discuss these two behaviors in detail.

The case displayed in Fig. 10 is characterized by $\alpha = 0.1$, and thus by a slowly decaying upper state, while the initial field amplitudes $\mathcal{G}_{g1}$, $\mathcal{G}_{g2}$, and $\tilde{\mathcal{G}}_{e1}$ are set well above their saturation values. In Fig. 10(a) the field $\mathcal{G}_{e2}$ is initially amplified until both the upper fields $\mathcal{G}_{e1}$ and $\mathcal{G}_{e2}$ reach a constant value along the medium. During the transient dynamics, the upper field amplitude $\mathcal{G}_{e1}$ and the lower field $\mathcal{G}_{g2}$ decrease while the lower field amplitude $\mathcal{G}_{g1}$ displays a slight increase around the transient end. This behavior is accompanied by a redistribution of population between the ground and the intermediate states while the excited state is depleted, see Fig. 10(c). Accordingly to Fig. 10(b), one observes that the phase reaches the value $\Theta = \pi$. Hence, the field $\mathcal{G}_{e2}$ is amplified until the upper state is depleted because of interference between the upper fields. From this point further the phase $\Theta = \pi$ is stable, until the lower field amplitudes go below saturation. The jump of the phase to the value 0 is an artifact due to all atoms being in the ground state.

In the case displayed in Fig. 11 the excited state is metastable and $\alpha = 0.01$. The initial field amplitudes $\mathcal{G}_{g1}$, $\mathcal{G}_{g2}$, and $\tilde{\mathcal{G}}_{e1}$ are set to the saturation value. In Fig. 11(a) the field $\mathcal{G}_{e2}$ is amplified while the upper field amplitude $\mathcal{G}_{e1}$ and both lower field amplitudes $\mathcal{G}_{g1}$ and $\mathcal{G}_{g2}$ decrease. In this transient dynamics the phase Θ reaches the value $\Theta = \pi$, see Fig. 11(b), and undergoes a jump to the value $\Theta = 0$ when $\mathcal{G}_{g2}$ vanishes. After this point the behavior changes and $\mathcal{G}_{g2}$ first increases and then decays slowly as a function of ξ in a way similar to $\mathcal{G}_{g1}$, while the upper field amplitudes remain constant. The final configuration supports a coherence between the excited and the ground state in a way similar to a cascade system. In particular, due to destructive interference, the fields are only weakly coupled to the transitions and the medium is semitransparent. This is also visible in Fig. 11(c) where we show that the population is redistributed between the ground and the excited states while the intermediate states are depleted. In this regime the medium is characterized by population inversion between the excited and the intermediate states.

IV. DISCUSSION AND CONCLUSIONS

We have investigated numerically light propagation in a medium of atoms whose electronic levels are resonantly driven by lasers in a $\diamondsuit$ configuration. Propagation is critically affected by the initial conditions of the input fields and show the tendency to reach configurations which minimize dissipation. A peculiar role is played by the relative phase Θ between the fields. In fact, it exhibits two fixed points, $\Theta = 0$ and $\Theta = \pi$, whose stability during propagation depends on the field amplitudes and on the ratio α between the rates of dissipation of excited and intermediate states. A generic input phase evolves, in general, to one of these values depending on the input amplitudes and α.

These two metastable responses are supported by two different types of atomic coherences. The response of the medium, corresponding to the phase $\Theta = 0$, is characterized by the formation of metastable atomic coherences typical of EIT-media. Similar behaviors have been observed for instance in [13, 14] and are analogous to the response predicted for light propagation in double-Λ media [9].

The response of the medium for the phase $\Theta = \pi$ is supported by a different type of interference which leads to a depletion of the upper state and to a perfect decoupling of the upper fields from the atom. For this value of the phase, the medium acts as if the atomic configuration were V-level scheme. In particular, this value of the phase appears to be the preferred value for the $\diamondsuit$ medium when the lower transitions are driven well above saturation. This behavior is novel to our knowledge and it is reminiscent of the phenomenon of suppression of spontaneous emission observed in four-wave mixing studies in atomic gases [23].

In general, the system offers a rich dynamics and several novel features due to atomic coherence which offer new perspectives in control techniques in quantum electronics. These could be studied in atomic gases where the ground state has no hyperfine multiplet, like e.g. alkali-earth isotopes which are currently investigated for atomic

clocks [19].

In the future we will extend our analysis to the case in which the transitions are not resonantly driven and we will address the asymptotic behavior of the system following the lines of recent works [24, 25].

Acknowledgments

The authors thank E. Arimondo, S. Barnett, R. Corbalan, and W.P. Schleich for discussions and helpful comments. G.M. and S.K.-S. acknowledge the warm hospitality of the Department of Physics at the University of Strathclyde. This work has been partially supported from the RTN-network CONQUEST and the scientific Exchange Programme Germany-Spain (HA2005-0001 and D/05/50582). G.M. is supported by the Spanish Ministerio de Educacion y Ciencias (Ramon-y-Cajal and FIS2005-08257-C02-01). S.F-A is supported by the Royal Society. G-L.O. thanks the CSDC of the University of Florence (Italy) for its kind hospitality.

APPENDIX A: MACROSCOPIC POLARIZATION IN THE SEMICLASSICAL LIMIT FOR THE ATOMIC MOTION

We consider the dynamics of the density matrix ϱ of the atomic internal and external degrees of freedom, where the center-of-mass degrees of freedom are treated as classical variables. Hence, the position $\mathbf{x}$ and momentum $\mathbf{p}$ are parameters, distributed according the function $w(\mathbf{x},\mathbf{p})$ which we assume to be stationary, with $\int \mathrm{d}\mathbf{x}\mathrm{d}\mathbf{p} w(\mathbf{x},\mathbf{p}) = N$ and N is the number of atoms. The spatial density of atoms $n(\mathbf{x})$ is found from $w(\mathbf{x},\mathbf{p})$ according to $\int \mathrm{d}\mathbf{p} w(\mathbf{x},\mathbf{p}) = n(\mathbf{x})$. In this work we assume uniform density, namely

$$n(\mathbf{x}) = n$$

with n constant. The master equation for the density matrix ϱ, at the point $(\mathbf{x},\mathbf{p})$ in phase space has the form

$$\dot{\varrho} = \frac{1}{\mathrm{i}\hbar}\left[H(\mathbf{x},\mathbf{p};t),\varrho\right] + \mathcal{L}\varrho \tag{A1}$$

where the Hamiltonian $H(\mathbf{x},\mathbf{p};t)$ contains the coherent dynamics of the atoms driven by the classical field,

$$H(\mathbf{x},\mathbf{p};t) = \frac{\mathbf{p}^2}{2M} + H(z,t) \tag{A2}$$

and $H(z,t)$ is defined in Eq. (15). The Liouvillian $\mathcal{L}$ describes the relaxation processes, which we consider here purely radiative. The corresponding macroscopic polarization has the form

$$\mathbf{P}(\mathbf{x},t) = \int \mathrm{d}\mathbf{p} w(\mathbf{x},\mathbf{p})\,\mathrm{Tr}\{\hat{\mathbf{d}}\varrho(\mathbf{x},\mathbf{p})\} \tag{A3}$$

Assuming that that atomic gas has been Doppler cooled, so that line broadening is homogeneous, the kinetic energy can be neglected in evaluating the atomic response to light. By integrating over $\mathbf{p}$ and x, y we hence obtain Eq. (14), whereby $\sigma(z) = \int \mathrm{d}\mathbf{p}\mathrm{d}x\mathrm{d}y w(\mathbf{x},\mathbf{p})\sigma(\mathbf{x},\mathbf{p})$, and polarization as in Eq. (2).

APPENDIX B: OPTICAL BLOCH EQUATIONS IN THE *PHASE*- REFERENCE FRAME

We consider Master Eq. (18) in the reference frame of the phase. With the notation $\tilde{\rho}_{e2} = \rho_{e2}\exp(-i\Theta)$, the corresponding optical Bloch equations are given by

$$\begin{aligned}
\dot{\rho}_{ee} &= i\frac{\Omega_{1e}}{2}(\rho_{1e}-\rho_{e1}) + i\frac{\Omega_{2e}}{2}(\tilde{\rho}_{2e} \\
&\quad -\tilde{\rho}_{e2}) - \gamma_e\rho_{ee} && \text{(B1)}\\
\dot{\rho}_{11} &= -i\frac{\Omega_{1e}}{2}(\rho_{1e}-\rho_{e1}) + i\frac{\Omega_{1g}}{2}(\rho_{g1}-\rho_{1g}) \\
&\quad +\frac{\gamma_e}{2}\rho_{ee} - \gamma_{1g}\rho_{11} && \text{(B2)}\\
\dot{\rho}_{22} &= -i\frac{\Omega_{2e}}{2}(\tilde{\rho}_{2e}-\tilde{\rho}_{e2}) + i\frac{\Omega_{2g}}{2}(\rho_{g2}-\rho_{2g}) \\
&\quad +\frac{\gamma_e}{2}\rho_{ee} - \gamma_{2g}\rho_{22} && \text{(B3)}\\
\dot{\rho}_{e1} &= \left(i\left(\Delta_1-\Delta_e\right) - \frac{\gamma_e+\gamma_{1g}}{2}\right)\rho_{e1} && \text{(B4)}\\
&\quad +i\frac{\Omega_{1e}}{2}(\rho_{11}-\rho_{ee}) + i\frac{\Omega_{2e}}{2}e^{i\Theta}\rho_{21} - i\frac{\Omega_{1g}}{2}\rho_{eg} \\
\dot{\tilde{\rho}}_{e2} &= \left(i\left(\Delta_2-\Delta_e\right) - \frac{\gamma_e+\gamma_{2g}}{2}\right)\tilde{\rho}_{e2} && \text{(B5)}\\
&\quad +i\frac{\Omega_{2e}}{2}(\rho_{22}-\rho_{ee}) + i\frac{\Omega_{1e}}{2}e^{-i\Theta}\rho_{12} - i\frac{\Omega_{2g}}{2}e^{-i\Theta}\rho_{eg} \\
\dot{\rho}_{1g} &= -\left(i\Delta_1 + \frac{\gamma_{1g}}{2}\right)\rho_{1g} + i\frac{\Omega_{1e}}{2}\rho_{eg} && \text{(B6)}\\
&\quad -i\frac{\Omega_{2g}}{2}\rho_{12} + i\frac{\Omega_{1g}}{2}(\rho_{gg}-\rho_{11}) \\
\dot{\rho}_{2g} &= -\left(i\Delta_2 + \frac{\gamma_{2g}}{2}\right)\rho_{2g} + i\frac{\Omega_{2e}}{2}e^{-i\Theta}\rho_{eg} && \text{(B7)}\\
&\quad -i\frac{\Omega_{1g}}{2}\rho_{21} + i\frac{\Omega_{2g}}{2}(\rho_{gg}-\rho_{22}) \\
\dot{\rho}_{12} &= \left(i\left(\Delta_2-\Delta_1\right) - \frac{\gamma_{1g}+\gamma_{2g}}{2}\right)\rho_{12} + i\frac{\Omega_{1e}}{2}e^{i\Theta}\tilde{\rho}_{e2} \\
&\quad +i\frac{\Omega_{1g}}{2}\rho_{g2} - i\frac{\Omega_{2g}}{2}\rho_{1g} - i\frac{\Omega_{2e}}{2}e^{i\Theta}\rho_{1e} && \text{(B8)}\\
\dot{\rho}_{eg} &= -\left(i\Delta_e + \frac{\gamma_e}{2}\right)\rho_{eg} + i\frac{\Omega_{1e}}{2}\rho_{1g} \\
&\quad +i\frac{\Omega_{2e}}{2}e^{i\Theta}\rho_{2g} - i\frac{\Omega_{1g}}{2}\rho_{e1} - i\frac{\Omega_{2g}}{2}e^{i\Theta}\tilde{\rho}_{e2}. && \text{(B9)}
\end{aligned}$$

where $\rho_{ij} = \rho^*_{ji}$, $\rho_{gg} = 1-\rho_{ee}-\rho_{11}-\rho_{22}$, and we have taken $\gamma_{e1} = \gamma_{e2} = \gamma_e/2$.

[1] S.E. Harris, Phys. Today **50**, 36 (1997); E. Arimondo, Prog. Opt. **35**, 259 (1996).

[2] D.A. Braje, V. Balic, S. Gida, G.Y. Yin, and S.E. Harris, Phys. Rev. Lett. **93**, 183601 (2004).

[3] V. Balic, D.A. Braje, P. Kolchin, G.Y. Yin, and S.E. Harris, Phys. Rev. Lett. **94**, 183601 (2005).

[4] M.D. Eisaman, L. Childress, A. André, F. Massou, A.S. Zibrov, and M.D. Lukin, Phys. Rev. Lett. **93**, 233602 (2004);

[5] J. Guo, P. R. Berman, B. Dubetsky, and G. Grynberg, Phys. Rev. A **46**, 1426 (1992).

[6] M. Vengalattore and M. Prentiss, Phys. Rev. Lett. **95**, 243601 (2005)

[7] S.J. Buckle, S.M. Barnett, P.L. Knight, M.A. Lauder, and D.T. Pegg, Optica Acta **33**, 1129 (1986).

[8] D.V. Kosachiov, B.G. Matisov, and Y.V. Rozhdestvensky, J. Phys. B: At. Mol. Opt. Phys. **25**, 2473 (1992).

[9] E.A. Korsunsky and D.V. Kosachiov, Phys. Rev. A **60**, 4996 (1999).

[10] G. Morigi, S. Franke-Arnold, G.-L. Oppo, Phys. Rev. A **66**, 053409 (2002)

[11] M.D. Lukin, P.R. Hemmer, and M.O. Scully, Adv. At. Mol. Opt. Phys. **42**, 347 (2000).

[12] H. Shpaisman, A.D. Wilson-Gordon, and H. Friedmann, Phys. Rev. A **70**, 063814 (2004); Phys. Rev. A **71**, 043812 (2005).

[13] W.E. van der Veer, R.J.J. van Diest, A. Dönszelmann, and H.B. van Linden van den Heuvell, Phys. Rev. Lett. **70**, 3243 (1993).

[14] W. Maichen, F. Renzoni, I. Mazets, E. Korsunsky, and L. Windholz, Phys. Rev. A **53**, 3444 (1996).

[15] A.J. Merriam, S.J. Sharpe, M. Shverdin, D. Manuszak, G.Y. Yin, and S.E. Harris, Phys. Rev. Lett. **84**, 5308 (2000).

[16] E.A. Korsunsky, N. Leinfellner, A. Huss, S. Baluschev, and L. Windholz, Phys. Rev. A **59**, 2302 (1999).

[17] A.F. Huss, R. Lammegger, C. Neureiter, E.A. Korsunsky, and L. Windholz, Phys. Rev. Lett. **93**, 223601 (2004).

[18] V.S. Malinovsky and I. R. Sola, Phys. Rev. Lett. **93**, 190502 (2004); Phys. Rev. A **70**, 042304 (2004); Phys. Rev. A **70**, 042305 (2004).

[19] R. Santra, E. Arimondo, T. Ido, C.H. Greene, and J. Ye, Phys. Rev. Lett. **94**, 173002 (2005); T. Ido, T.H. Loftus, M.M. Boyd, A.D. Ludlow, K.W. Holman, and J. Ye, Phys. Rev. Lett. **94**, 153001 (2005).

[20] M.O. Scully and M.S. Zubairy, *Quantum Optics*, Cambridge University Press ed. (Cambridge 1997).

[21] This behavior may not seem obvious for $\alpha \to \infty$, but it becomes evident after rescaling the field amplitudes, Eq. (9), with the linewidth γ_e and then letting $\gamma_{jg} \to 0$.

[22] R. M. Whitley and C. R. Stroud, Jr., Phys. Rev. A **14**, 1498 (1976).

[23] M.S. Malcuit, D.J. Gauthier, and R.W. Boyd, Phys. Rev. Lett. **55**, 1086 (1985); R.W. Boyd, M.S. Malcuit, D.J. Gauthier, and K. Rzażewski, Phys. Rev. A **35**, 1648 (1987).

[24] E.A. Korsunsky and M. Fleischhauer, Phys. Rev. A **66**, 033808 (2002).

[25] M.T. Johnsson and M. Fleischhauer, Phys. Rev. A **66**, 043808 (2002).

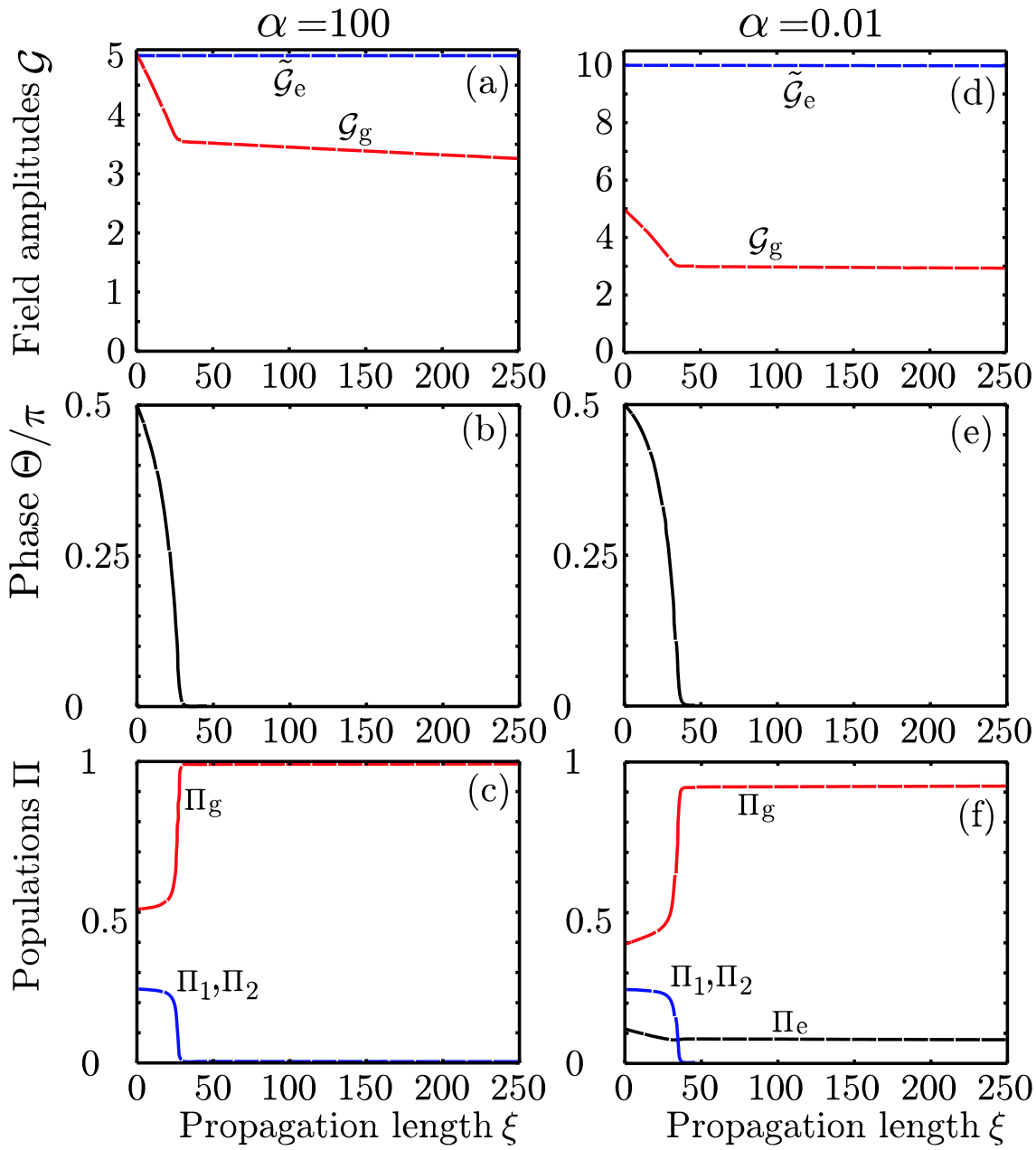

FIG. 8: (color online) (a) Field amplitudes $\mathcal{G}_g$ (red) and $\tilde{\mathcal{G}}_e$ (blue line), (b) relative phase Θ and (c) populations of the electronic levels Π_g(red), Π_1, Π_2 (blue), Π_e (black) as a function of the propagation length ξ, for $\Theta(0) = \pi/2$, $\alpha = 100$, $\mathcal{G}_g(0) = 5$ and $\tilde{\mathcal{G}}_e(0) = 5$. (d), (e), (f): same as (a), (b) and (c), respectively, for $\Theta(0) = \pi/2$, $\alpha = 0.01$, $\mathcal{G}_g(0) = 5$ and $\tilde{\mathcal{G}}_e(0) = 10$.

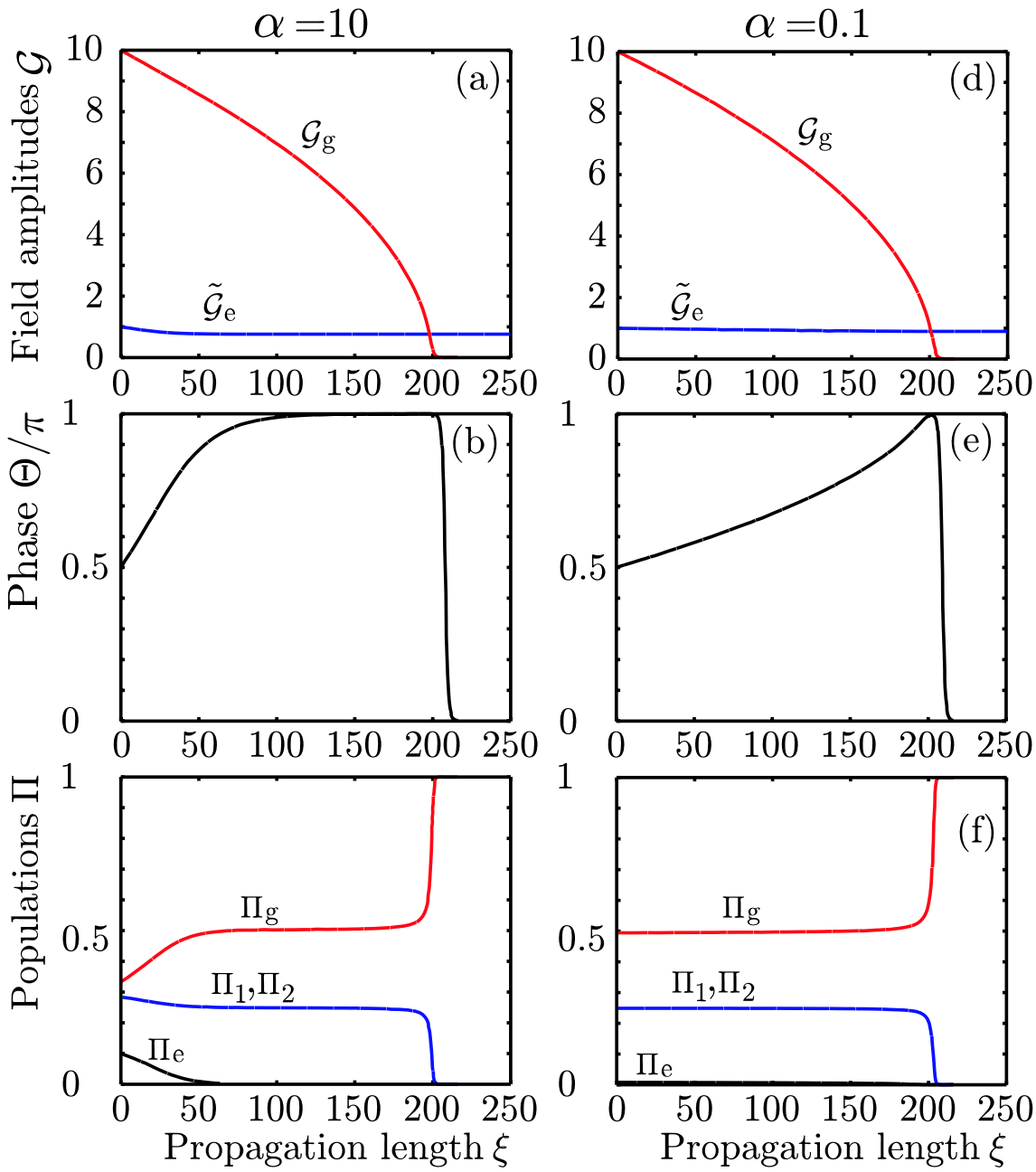

FIG. 9: (color online) (a) Field amplitudes $\mathcal{G}_g$ (red) and $\tilde{\mathcal{G}}_e$ (blue), (b) relative phase Θ and (c) populations of the electronic levels Π_g (red), Π_1 (blue), Π_2 (blue) and Π_e (black) as a function of the propagation length ξ, for $\Theta(0) = \pi/2$, $\alpha = 10$, $\mathcal{G}_g(0) = 10$ and $\tilde{\mathcal{G}}_e(0) = 1$. (d), (e), (f): same as (a), (b) and (c), respectively, for $\Theta(0) = \pi/2$, $\alpha = 0.1$, $\mathcal{G}_g(0) = 10$ and $\tilde{\mathcal{G}}_e(0) = 1$.

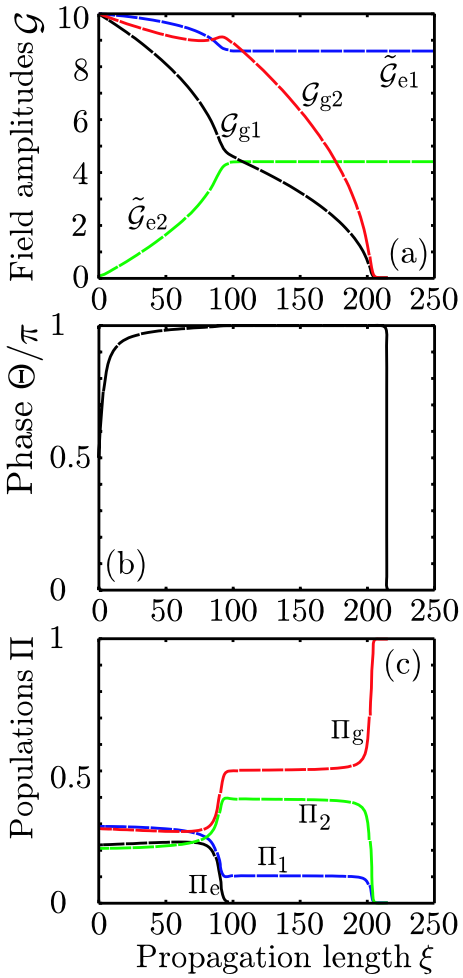

FIG. 10: (color online) (a) Field amplitudes $\mathcal{G}_{g1}$ (black), $\mathcal{G}_{g2}$(red), $\tilde{\mathcal{G}}_{e1}$ (blue) and $\tilde{\mathcal{G}}$ (green), (b) relative phase Θ and (c) populations of the electronic levels Π_g(red), Π_1(blue), Π_2(green), Π_e (black) as a function of the propagation length ξ, for $\Theta(0) = \pi/2$, $\alpha = 0.1$, $\mathcal{G}_{g1}(0) = \mathcal{G}_{g2}(0) = 10$, $\mathcal{G}_{e1}(0) = 10$, and $\mathcal{G}_{e2}(0) = 0.1$.

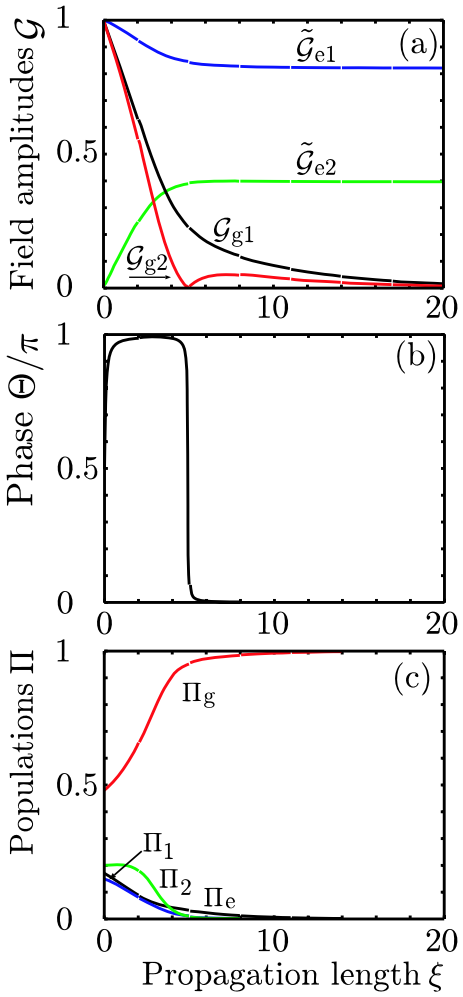

FIG. 11: (color online) (a) Field amplitudes $\mathcal{G}_{g1}$ (black), $\mathcal{G}_{g2}$(red), $\tilde{\mathcal{G}}_{e1}$ (blue) and $\tilde{\mathcal{G}}_{e2}$ (green), (b) relative phase Θ and (c) populations of the electronic levels Π_g(red), Π_1(blue), Π_2(green) and Π_e (black) as a function of the propagation length ξ, for $\Theta(0) = \pi/2$, $\alpha = 0.01$, $\mathcal{G}_{g1}(0) = \mathcal{G}_{g2}(0) = 1$, $\tilde{\mathcal{G}}_{e1}(0) = 1$, and $\tilde{\mathcal{G}}_{e2}(0) = 0.01$.